

# Polysulfide Anions as Visible Light Photoredox Catalysts for Aryl Cross-Couplings

Haoyu Li, Xinxin Tang,<sup>§</sup> Jia Hao Pang,<sup>§</sup> Xiangyang Wu, Edwin K. L. Yeow, Jie Wu, and Shunsuke Chiba\*



Cite This: *J. Am. Chem. Soc.* 2021, 143, 481–487



Read Online

ACCESS |



Metrics & More

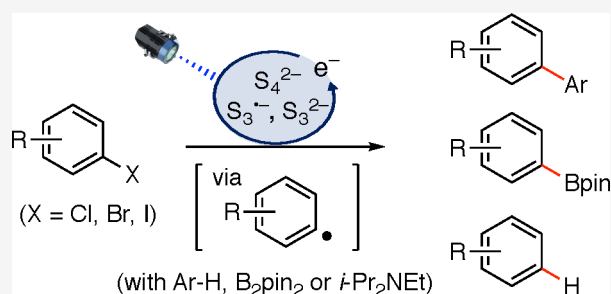


Article Recommendations



Supporting Information

**ABSTRACT:** Polysulfide anions are endowed with unique redox properties, attracting considerable attentions for their applications in alkali metals–sulfur batteries. However, the employment of these anionic species in redox catalysis for small molecule synthesis remains underdeveloped due to their moderate–poor electrochemical potential in the ground state, whereas some of them are characterized by photoabsorptions in visible spectral regions. Herein, we disclose the use of polysulfide anions as visible light photoredox catalysts for aryl cross-coupling reactions. The reaction design enables single-electron reduction of aryl halides upon the photoexcitation of tetrasulfide dianions ( $S_4^{2-}$ ). The resulting aryl radicals are engaged in (hetero)-biaryl cross-coupling, borylation, and hydrogenation in a redox catalytic regime involving  $S_4^{\bullet-}/S_4^{2-}$  and  $S_3^{\bullet-}/S_3^{2-}$  redox couples.



## INTRODUCTION

Visible light photoredox catalysis has advanced in the state-of-the-art chemical synthesis, enabling us to harness lower energy visible light to productively drive various types of useful molecular transformations.<sup>1</sup> Homogeneous photocatalysts such as ruthenium-/iridium-based polypyridyl complexes or organic dyes could be excited under irradiation with visible light, inducing a single-electron transfer (SET) to or from organic substrates to provide reactive open-shell radical intermediates. The employment of heterogeneous semiconductor as a redox active chromophore for the synthesis of complex molecules has recently offered another contemporary trend in photoredox catalysis.<sup>2</sup> Nonetheless, the further development of new photocatalysts based on inexpensive and abundant elements that can perform productive bond formation processes in a highly efficient fashion is of prominent interest.

Sulfur is known to form various catenated homoatomic polysulfide dianions  $S_x^{2-}$  (typically,  $x = 2-8$ ) and a persistent radical anion  $S_3^{\bullet-}$ , which is known as a blue chromophore in ultramarine blues.<sup>3</sup> In seeking the development of alkali metals–sulfur batteries, the chemical reactivity and redox characters of polysulfide anions have been elucidated in detail.<sup>4</sup> Polysulfide anions undergo complicated redox, dissociative, and disproportionation processes in the solution states to afford an equilibrium mixture of multiple polysulfide anions, and their steady states depend majorly on the solvents. The *in situ* spectroelectrochemical studies on the reduction of octasulfur ( $S_8$ ) identified the ground state redox couples of  $S_3^{\bullet-}/S_3^{2-}$  and  $S_4^{\bullet-}/S_4^{2-}$ , and their electrochemical potentials are estimated at around  $-1.35$  and  $-0.85$  V, respectively,

versus saturated calomel electrode (SCE) in dimethylformamide (DMF)<sup>5</sup> (Scheme 1 A). However, the employment of these homoatomic sulfide anions in redox catalysis that engages organic electrophores in the radical-mediated reactions remains an unmet challenge. Nonetheless, their electrochemical potentials dictate that they are incapable of inducing the single-electron reduction of unactivated organic electrophores of highly negative reduction potentials such as aryl halides [ $E_{\text{red}} < 1.9$  V (vs SCE)].<sup>6</sup> On the contrary, these species show a characteristic absorbance in the ultraviolet–visible (UV–vis) spectroscopy and some of them are observed in the visible spectral regions. For example, a degassed solution of cheap and readily available potassium polysulfide ( $K_2S_x$ , US \$0.12 per gram) in dimethyl sulfoxide (DMSO) shows a blue color and its steady-state UV–vis absorption spectrum indicates the presence of persistent  $S_3^{\bullet-}$  ( $\lambda_{\text{max}}$  at 618 nm with a wide bandwidth ranging from 450 to 800 nm),  $S_4^{2-}$  ( $\lambda_{\text{max}}$  at 436 and 333 nm), and  $S_3^{2-}$  ( $\lambda_{\text{max}}$  at 273 nm) (Scheme 1 B). We posited that on the basis of the redox potentials and visible photon absorptions of  $S_4^{2-}$  and  $S_3^{\bullet-}$  in their ground state, oxidizable  $S_4^{2-}$  could potentially serve as a photoexcited reductant whereas reducible  $S_3^{\bullet-}$  could function as a photoexcited oxidant.<sup>1f</sup> Therefore, we anticipated that these

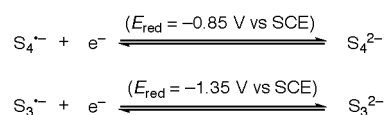
Received: November 15, 2020

Published: December 23, 2020

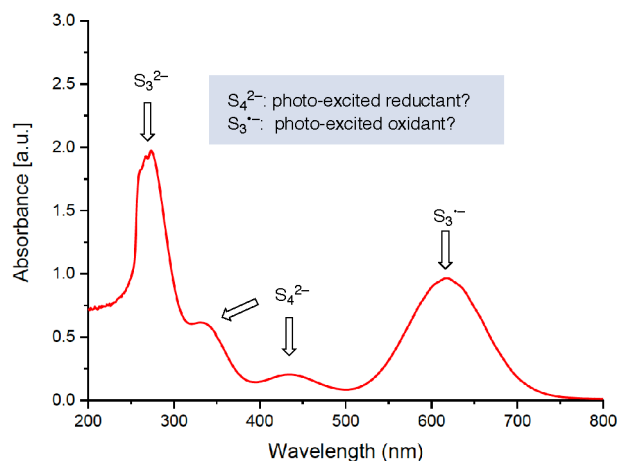


### Scheme 1. Redox Potential and UV-vis Absorption of Polysulfide Anions

#### A. Redox potential of $S_4^{2-}/S_4^{3-}$ and $S_3^{2-}/S_3^{3-}$ redox couples



#### B. UV-vis spectrum of potassium polysulfide ( $K_2S_x$ ) in DMSO



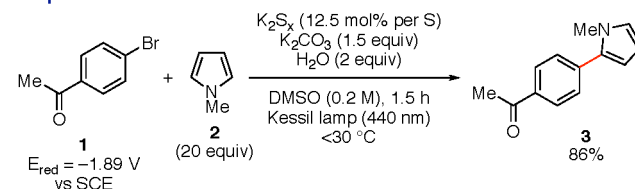
polysulfide anions could be engaged seamlessly in SET-driven radical-mediated processes in a redox catalytic manifold under visible light irradiation. Herein, we report the use of polysulfide anions  $S_4^{2-}$  and  $S_3^{3-}$  as photoredox catalysts for aryl cross-coupling reactions. The reaction design leverages the photoexcitation of  $S_4^{2-}$  to induce the single-electron reduction of aryl halides, having reduction potentials ( $E_{\text{red}}$ ) as low as  $-2.4 \text{ V}$  (vs SCE). The resulting aryl radicals are engaged in (hetero)biaryl cross-coupling, borylation, and hydrogenation in a redox catalytic regime where the redox interplay between  $S_4^{3-}/S_4^{2-}$  and  $S_3^{3-}/S_3^{2-}$  redox couples enables the redox-neutral catalytic turnover.

## RESULTS

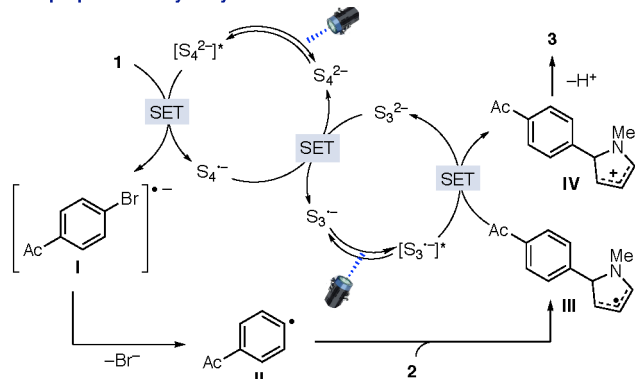
**Development of Biaryl Cross-Coupling.** At the outset of the project, we explored if the DMSO solution of  $K_2S_x$  containing  $S_3^{3-}$ ,  $S_4^{2-}$ , and  $S_3^{2-}$  could engage aryl halides in radical coupling reactions under visible light irradiation. We selected to investigate a heterobiaryl coupling of 4'-bromoacetophenone (**1**,  $E_{\text{red}} = -1.89 \text{ V}$  vs SCE)<sup>6</sup> as an electrophore with *N*-methylpyrrole (**2**) as a radical acceptor. The current state-of-the-art strategies for such a radical-based biaryl cross-coupling<sup>7</sup> leverage highly reducing photoexcited radical anions of polyaromatic hydrocarbons as a photoexcited reductant. In particular, consecutive photoelectron-transfer processes shown by König<sup>8</sup> and electrophotocatalytic strategies detailed by Lambert and Lin<sup>9a</sup> and Wickens<sup>9b</sup> have successfully generated excited radical anions. The leveraging of readily accessible  $\alpha$ -aminoalkyl radicals for hydrogen-atom transfer agents was recently proven useful to promote aryl cross-coupling by Leonori,<sup>10a</sup> while the inherent net-oxidative nature of the process necessitates the use of a stoichiometric amount of the oxidant. More recently, the same group revealed that  $\alpha$ -aminoalkyl radicals serve as an initiator and a chain carrier for the aryl cross-coupling between aryl halides (especially aryl iodides) and pyrroles.<sup>10b</sup> Our optimization of the reaction conditions revealed that the irradiation with blue light ( $\lambda_{\text{max}} =$

### Scheme 2. Photoredox Biaryl Cross-Coupling Catalyzed by $K_2S_x$

#### A. Optimized reaction conditions<sup>a</sup>

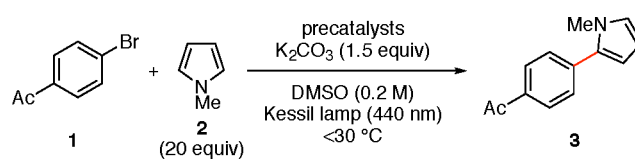


#### B. A proposed catalytic cycle



<sup>a</sup>Reaction conditions: **1** (0.5 mmol), **2** (20 equiv),  $K_2S_x$  (12.5 mol % per S) with  $H_2O$  (2 equiv),  $K_2CO_3$  (1.5 equiv), DMSO (2.5 mL), 440 nm light (Kessil lamp),  $< 30^\circ \text{C}$ . Isolated yield of **3** was recorded.

**Table 1. Screening of Precatalysts for Polysulfide Anions<sup>a</sup>**



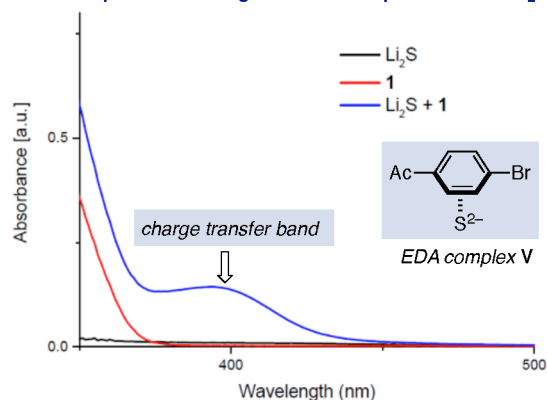
entry	precatalysts	time (h)	yield of <b>3</b> (%) <sup>b</sup>
1	$K_2S_x$ (12.5 mol %/S) + $H_2O$ (2 equiv)	1.5	92 (86) <sup>c</sup>
2	$S_8$ (10 mol %/S) + NaOt-Bu (10 mol %)	3	85
3	$Li_2S$ (10 mol %)	2	88
4	<i>i</i> -Pr <sub>3</sub> SiSH (10 mol %)	2	82

<sup>a</sup>Reaction conditions: **1** (0.5 mmol), **2** (20 equiv), precatalysts,  $K_2CO_3$  (1.5 equiv), DMSO (2.5 mL), 440 nm light (Kessil lamp),  $< 30^\circ \text{C}$ . <sup>b</sup><sup>1</sup>H NMR yields based on the internal standard. <sup>c</sup>Isolated yield.

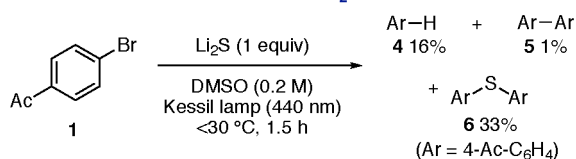
440 nm) to the mixture of **1** and **2** in the presence of  $K_2S_x$  (12.5 mol % per S atom), potassium carbonate ( $K_2CO_3$ , 1.5 equiv), and water ( $H_2O$ , 2 equiv) in DMSO enabled an efficient coupling to afford heterobiaryl **3** in 86% yield within 1.5 h (Scheme 2A). The control experiments indicated that  $K_2S_x$ , the irradiation with blue light, and a buffer ( $K_2CO_3$ ) are all essential for the process, and the reaction is hampered under an air atmosphere (see the Supporting Information (SI), Table S1). The following synergistic catalytic cycle involving  $S_4^{2-}/S_4^{3-}$  and  $S_3^{2-}/S_3^{3-}$  redox couples is proposed (Scheme 2B). Photoexcitation by 440 nm light endows  $S_4^{2-}$  with highly reducing potential in its excited state,<sup>11</sup> allowing for single-electron reduction of **1** to form arene radical anion I along with generation of  $S_4^{3-}$ . The single-electron reduction of reducible  $S_4^{3-}$  by concomitant ground-state oxidizable  $S_3^{2-}$  allows for the regeneration of ground-state  $S_4^{2-}$ . Meanwhile, the resulting arene radical anion I undergoes mesolysis of the carbon-

### Scheme 3. Bottom-up Generation of Polysulfide Anions from Mono-Sulfides $\text{Li}_2\text{S}$ and $i\text{-Pr}_3\text{SiSH}$

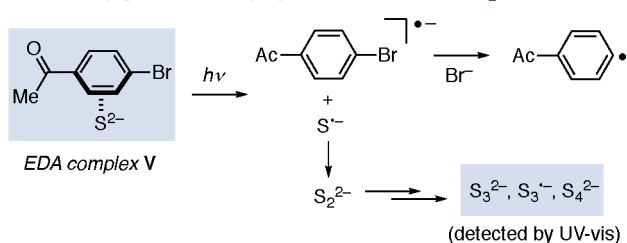
#### A. UV-vis spectra for charge-transfer complex of 1 with $\text{Li}_2\text{S}$ .



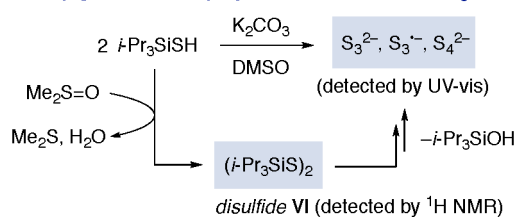
#### B. A stoichiometric reaction of 1 with $\text{Li}_2\text{S}$



#### C. Bottom-up generation of polysulfide anions from $\text{Li}_2\text{S}$



#### D. Bottom-up generation of polysulfide anions from $i\text{-Pr}_3\text{SiSH}$



halogen bond to afford aryl radical **II**,<sup>12</sup> which adds onto **2** to form the radical intermediate **III**. Single-electron oxidation of **III** by photoexcited  $\text{S}_3^{\bullet-}$  followed by deprotonation liberates **3** and ground-state  $\text{S}_3^{2-}$ .<sup>13</sup> We measured the quantum yield for the formation of **3** under the optimized reaction conditions, which was determined as  $\Phi = 0.07$ . This implicates that a possibility of the radical chain process<sup>10b</sup> is less likely and supports the proposed photoredox catalytic cycle.

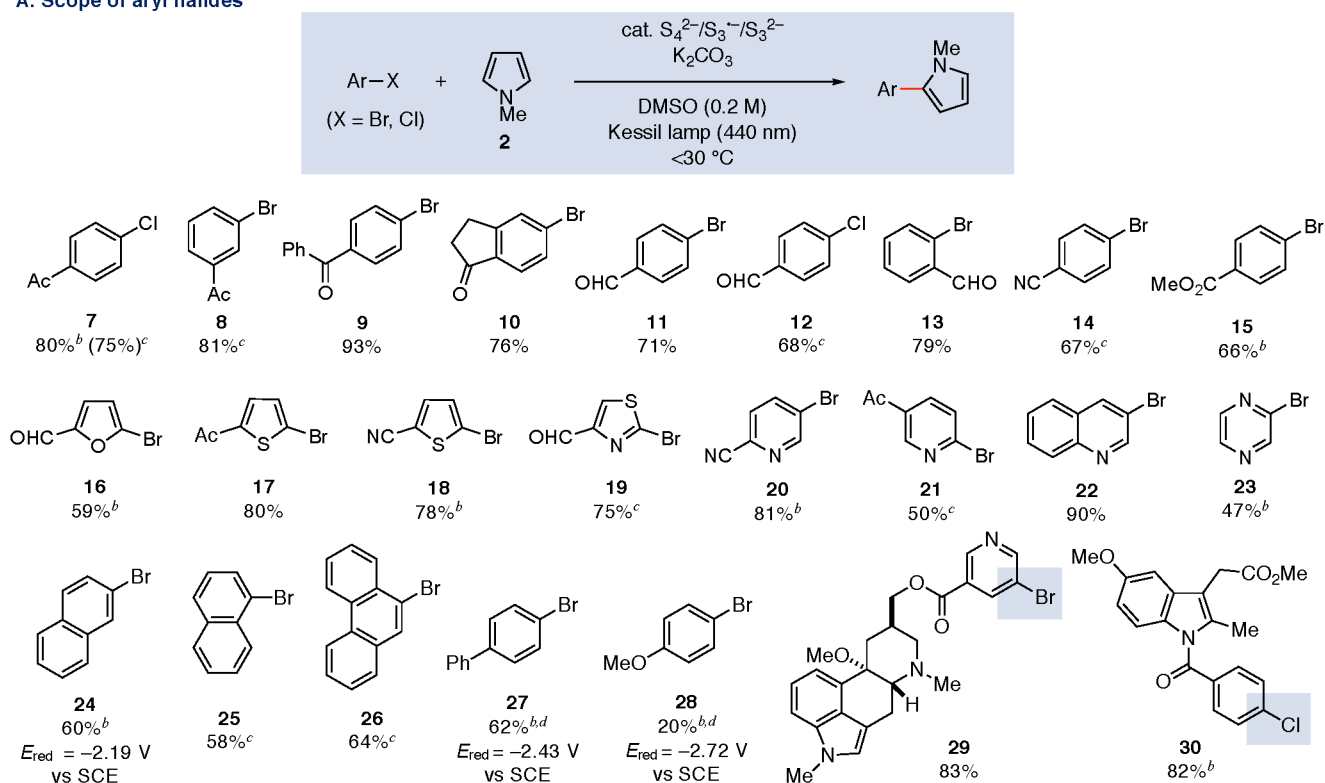
**Evaluation of Precatalysts.** We next screened the precatalysts of the polysulfide anions in the cross-coupling between **1** and **2** (Table 1). The top-down generation of polysulfide anions through the reductive fragmentation of octasulfur ( $\text{S}_8$ )<sup>14</sup> in the presence of sodium *tert*-butoxide ( $\text{NaOt-Bu}$ ) in DMSO was amenable for the productive cross-coupling (entry 2). We also found that the bottom-up generation of polysulfide anions from monosulfide species is suitable for the catalysis. For example, the use of dilithium sulfide ( $\text{Li}_2\text{S}$ , 10 mol %) as a precatalyst led to a full conversion of **1** within 2 h to afford **3** in 88% yield (entry 3). Similarly, neutral triisopropylsilylthiol ( $i\text{-Pr}_3\text{SiSH}$ ), which has commonly

been utilized as a hydrogen-atom transfer catalyst,<sup>15</sup> could also perform as a promising precatalyst (entry 4).

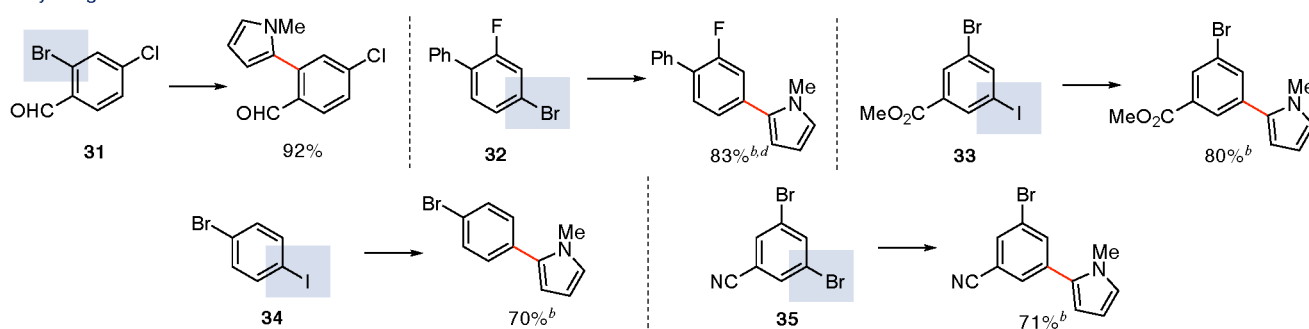
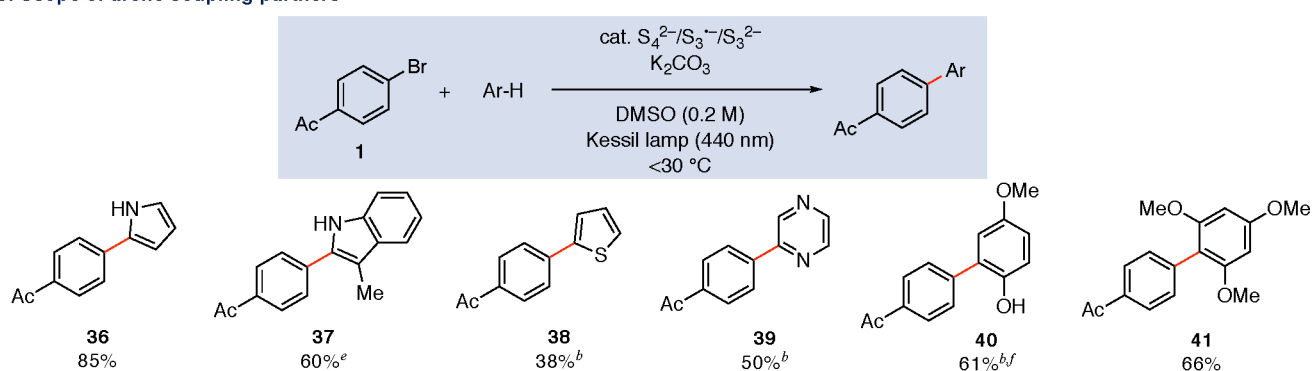
These monosulfides ( $\text{Li}_2\text{S}$  and  $i\text{-Pr}_3\text{SiSH}$ ) neither showed absorption at the visible region nor facilitated the cross-coupling reaction under the dark conditions due to an insufficient oxidation potential of monosulfide ions ( $E_{\text{ox}}$  of  $\text{S}^{2-} = -0.76$  V vs SCE)<sup>16</sup> (see the SI, Figures S13–S15). On the contrary, a charge-transfer absorption band was observed from the mixture of **1** and  $\text{Li}_2\text{S}$  (Scheme 3A) and the irradiation with blue light (440 nm) to a mixture of **1** and  $\text{Li}_2\text{S}$  (in 1:1 molar ratio) in DMSO formed acetophenone (**4**), biaryl **5**, and diaryl sulfide **6**, all of which could be derived from the corresponding aryl radical (Scheme 3B and Figure S4). We propose that  $\text{Li}_2\text{S}$  triggers the cross-coupling process through the formation of electron-donor-acceptor (EDA) complex V with **1**, which induces single-electron transfer upon the irradiation with visible light to produce a radical ion pair (Scheme 3C).<sup>17</sup> The resulting radical anion of **1** undergoes cleavage of the C–Br bond to form the aryl radical, whereas a simultaneously formed monosulfide anion radical ( $\text{S}^{\bullet-}$ ) undergoes dimerization to form a disulfide dianion ( $\text{S}_2^{2-}$ ) and its subsequent disproportionation generates the higher order photoredox active polysulfides,<sup>18</sup> which promote the photocatalytic turnover further. Interestingly,  $i\text{-Pr}_3\text{SiSH}$  might initiate the bottom-up formation of polysulfide anions in a different manner. We observed that the treatment of  $i\text{-Pr}_3\text{SiSH}$  with  $\text{K}_2\text{CO}_3$  in DMSO immediately stains the solution blue, and the UV-vis absorption spectroscopy unambiguously indicated the generation of polysulfide anions ( $\text{S}_3^{\bullet-}$ ,  $\text{S}_4^{2-}$ , and  $\text{S}_3^{2-}$ ) (Figure S16). The nuclear magnetic resonance (NMR) spectroscopy showed the formation of disulfide ( $i\text{-Pr}_3\text{SiS}$ )<sub>2</sub> **VI** in the solution (Figure S5). Therefore, we postulated that DMSO functions as an oxidant<sup>19</sup> to promote the desilylative oligomerization of  $i\text{-Pr}_3\text{SiSH}$  to the higher order polysulfides *via* disulfide **VI** (Scheme 3D). The capability of disulfide **VI** as the catalyst was ascertained as it performed the productive cross-coupling (Table S2).

**Substrate Scope on Biaryl Cross-Coupling.** We found that this photoredox protocol with polysulfide anions is capable of engaging a wide range of aryl halides for the (hetero)biaryl coupling (Scheme 4A). We first studied the reactivity of 4'-chloroacetophenone (**7**), having a reductively inert C–Cl bond.<sup>20</sup> We observed a diminished efficiency in the reaction with  $\text{K}_2\text{S}_x$  (12.5 mol % per S atom), resulting in an incomplete conversion of **7** (60%) even after irradiation for 22 h (Table S3). We found that the use of  $\text{Li}_2\text{S}$  and  $i\text{-Pr}_3\text{SiSH}$  results in the completion of the process within 4 h to give coupling product **3** in 80% and 75% yields, respectively. These outcomes suggested that a bottom-up preparation of the polysulfide anions from mono sulfides would provide more productive reactivity especially for reductively recalcitrant aryl halides. The method allows for the installation of various polar- $\pi$  electron-withdrawing groups susceptible to reductive reaction conditions, such as ketone (**7–10**), aldehyde (**11–13**), nitrile (**14**), and ester (**15**). The protocol could successfully engage five-membered ring heteroaryl halides based on furan (**16**), thiophene (**17, 18**), and thiazole (**19**). The chemistry was also extended to functionalize six-membered ring heteroaryl halides such as pyridine (**20, 21**), quinoline (**22**), and pyrazine (**23**). We also found that nonactivated aryl halides having a highly negative reduction potential ( $E_{\text{red}} > -2.4$  V vs SCE)<sup>21</sup> are suitable substrates (**24–27**). In these cases, the employment of  $\text{Li}_2\text{S}$  or  $i\text{-Pr}_3\text{SiSH}$  (10

## Scheme 4. Reaction Scope on (Hetero)biaryl Cross-Coupling

A. Scope of aryl halides<sup>a</sup>

## Polyhalogenated aromatics

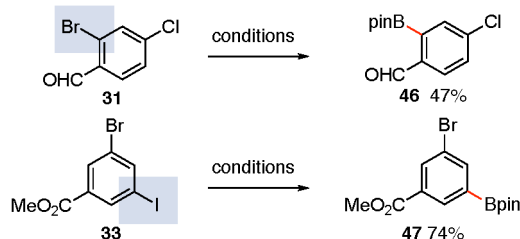
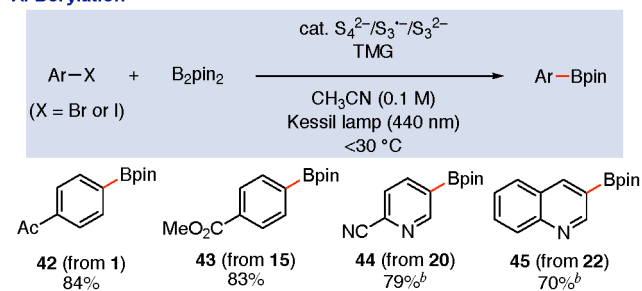
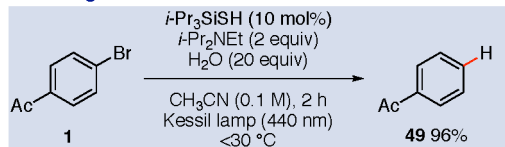
B. Scope of arene coupling partners<sup>a</sup>

<sup>a</sup>Reaction conditions: substrates (0.5 mmol), coupling partners (20 equiv), K<sub>2</sub>S<sub>x</sub> (12.5 mol % per S) with H<sub>2</sub>O (2 equiv), K<sub>2</sub>CO<sub>3</sub> (1.5 equiv), DMSO (2.5 mL), 440 nm light (Kessil lamp), < 30 °C. Isolated yields of the products were recorded. <sup>b</sup>Precatalyst: Li<sub>2</sub>S (10 mol %). <sup>c</sup>Precatalyst: *i*-Pr<sub>3</sub>SiSH (10 mol %). <sup>d</sup>390 nm light. <sup>e</sup>Ten equiv of 3-methylindole was used. <sup>f</sup>The reaction was run with 5 equiv of 4-methoxyphenol and 5 equiv of NaOt-Bu.

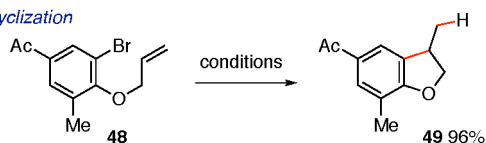
mol %) as a precatalyst was optimal. However, the reaction of reductively more inert 4-bromoanisole (28) (E<sub>red</sub> = -2.72 V vs

SCE)<sup>22</sup> was sluggish. This protocol was found to be capable in the functionalization of nicergoline (29) and indomethacin

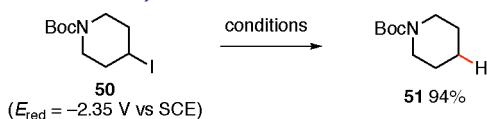
## Scheme 5. Borylation and Hydrodehalogenation

A. Borylation<sup>a</sup>B. Hydrodehalogenation<sup>c</sup>

## • radical cyclization



## • hydrodeiodination of alkyl iodide



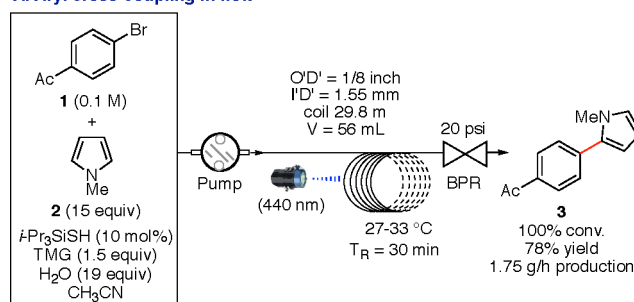
<sup>a</sup>Reaction conditions: substrates (0.5 mmol), B<sub>2</sub>pin<sub>2</sub> (2 equiv), K<sub>2</sub>S<sub>x</sub> (12.5 mol % per S), TMG (1.5 equiv), CH<sub>3</sub>CN (5 mL), 440 nm light (Kessil lamp), < 30 °C. Isolated yields of the products were recorded.

<sup>b</sup>Precatalyst: *i*-Pr<sub>3</sub>SiSH (10 mol %). <sup>c</sup>substrates (0.5 mmol), *i*-Pr<sub>2</sub>NET (2 equiv), *i*-Pr<sub>3</sub>SiSH (10 mol %), H<sub>2</sub>O (20 equiv), CH<sub>3</sub>CN (5 mL), 440 nm light (Kessil lamp), < 30 °C.

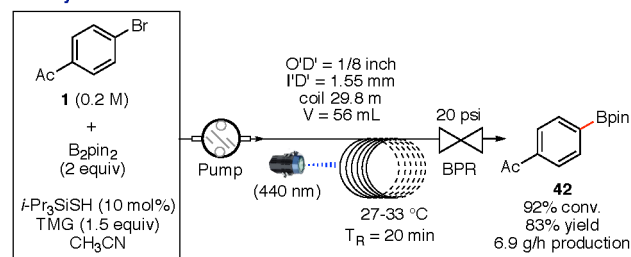
methyl ester (30) without damaging the other functional groups in these substrates. Finally, we explored if polyhalogenated aromatic substrates could be engaged in chemo-selective cross-coupling processes. We were pleased to observe that 2-bromo-4-chlorobenzaldehyde (31) was selectively functionalized on the C–Br bond. Similarly, the coupling reaction of 4-bromo-2-fluoro-1,1'-biphenyl (32) occurs selectively at the C–Br bond. A more reactive C–I bond<sup>23</sup> could be functionalized selectively in the reactions of methyl 3-bromo-5-iodobenzoate (33) and 1-bromo-4-iodobenzene (34). Moreover, 3,5-dibromobenzonitrile (35) was found to undergo single functionalization at one of the C–Br bonds. The scope with respect to the trapping (hetero)arenes was next evaluated (Scheme 4B). The use of N–H pyrrole (36) and indole (37) was found to be optimal, while the coupling with thiophene (38) resulted in moderate efficiency. The protocol enables the Minisci type-coupling with pyrazine (39).

Scheme 6. Scale-up in Flow<sup>a</sup>

## A. Aryl cross-coupling in flow



## B. Borylation in flow



<sup>a</sup>O'D' = outer diameter; I'D' = inner diameter; T<sub>R</sub> = residence time; V = volume of the micro-tubing reactor; BPR = back pressure regulator.

Electron-rich benzenes (40, 41) were also found to be compatible as a coupling partner.

**Development of Borylation and Hydrodehalogenation.** The synthetic utility of this polysulfide anions-based photoredox catalysis was further extended to the dehaloborylation reaction by employing bis(pinacolato)diboron (B<sub>2</sub>pin<sub>2</sub>) as the radical trapping reagents (Scheme 5A and Table S4).<sup>24,25</sup> The optimization for the borylation of 4'-bromoacetophenone (1) with K<sub>2</sub>S<sub>x</sub> as a precatalyst led to the identification of tetramethylguanidine (TMG) and acetonitrile (CH<sub>3</sub>CN) as the optimal base and solvent, respectively, delivering pinacol arylboronate 42 in 84% yield within 1.5 h. This protocol was found to be applicable to the borylation of various functionalized haloarenes (43–47). We also found that the protocol is amenable to hydrodebromination of 1 using diisopropylethylamine (*i*-Pr<sub>2</sub>NET) as a hydrogen donor, providing acetophenone (4) in 96% yield within 2 h (Scheme 5B and Table S5).<sup>22,26,27</sup> The identified reaction conditions were capable of reductive radical cyclization of 48 to dihydrobenzofuran 49 and hydrodeiodination of secondary alkyl iodide 50 ( $E_{\text{red}} = -2.35 \text{ V}$ )<sup>10a</sup> to 51.

**Scale-up in Flow.** These batch photoredox processes catalyzed by the polysulfide anions stimulated us to explore the scalability of the heterobiaryl cross-coupling and borylation in flow (Scheme 6). The cross-coupling between 1 and 2 was efficiently promoted in a homogeneous system using *i*-Pr<sub>3</sub>SiSH as a precatalyst and tetramethylguanidine (TMG) as a base in an operationally simple microtubing continuous-flow reactor<sup>28</sup> (Figure S8). The desired product 3 was delivered at a 1.75 g/hour production rate (78%) with 30 min as the residence time (Scheme 6A). The debromo-borylation of 1 could also be performed in the same flow reactor to afford 42 at a 6.9 g/hour production rate (83%) with 20 min as the residence time (Scheme 6B).

## CONCLUSION

The key enabling advance in the present method takes advantage of unique reactivity of the polysulfide anions as photoredox catalysts, which are capable of engaging a wide range of aryl halides in productive radical cross-coupling chemistry. We anticipate that the broad scope with wide functional group compatibility, operational simplicity, and scalability in flow would bring useful and practical applications of this catalysis strategy in various fields.

## ASSOCIATED CONTENT

### Supporting Information

The Supporting Information is available free of charge on the ACS Publications Web site. Procedures and characterization data (PDF) The Supporting Information is available free of charge at <https://pubs.acs.org/doi/10.1021/jacs.0c11968>.

Discussions of characterization methods used, reaction optimization, experimental protocols, determination of the quantum yield, light on/off experiment, stoichiometric reactions, characterization of products, proposed mechanisms, scale up in flow, and preliminary mechanistic investigation, figures of emission spectra, batch reaction setup, reaction profiles, proposed mechanisms, NMR spectra, proposed catalytic cycles, absorption spectra, UV-vis spectra, steady state fluorescence spectrum, lifetime decay profiles, and reaction pathways, and tables of reaction optimizations (PDF)

## AUTHOR INFORMATION

### Corresponding Author

Shunsuke Chiba – Division of Chemistry and Biological Chemistry, School of Physical and Mathematical Sciences, Nanyang Technological University, 637371, Singapore; [orcid.org/0000-0003-2039-023X](https://orcid.org/0000-0003-2039-023X); Email: [shunsuke@ntu.edu.sg](mailto:shunsuke@ntu.edu.sg)

### Authors

Haoyu Li – Division of Chemistry and Biological Chemistry, School of Physical and Mathematical Sciences, Nanyang Technological University, 637371, Singapore

Xinxin Tang – Department of Chemistry, National University of Singapore, 117543, Singapore

Jia Hao Pang – Division of Chemistry and Biological Chemistry, School of Physical and Mathematical Sciences, Nanyang Technological University, 637371, Singapore

Xiangyang Wu – Division of Chemistry and Biological Chemistry, School of Physical and Mathematical Sciences, Nanyang Technological University, 637371, Singapore

Edwin K. L. Yeow – Division of Chemistry and Biological Chemistry, School of Physical and Mathematical Sciences, Nanyang Technological University, 637371, Singapore; [orcid.org/0000-0003-0290-4882](https://orcid.org/0000-0003-0290-4882)

Jie Wu – Department of Chemistry, National University of Singapore, 117543, Singapore; [orcid.org/0000-0002-9865-180X](https://orcid.org/0000-0002-9865-180X)

Complete contact information is available at: <https://pubs.acs.org/doi/10.1021/jacs.0c11968>

### Author Contributions

<sup>§</sup>X.T. and J.H.P. contributed equally.

## Notes

The authors declare no competing financial interest.

## ACKNOWLEDGMENTS

Financial support was provided by Pharma Innovation Programme Singapore (A\*STAR, SERC A19B3a0014). The authors would like to thank Han Sen Soo (NTU Singapore), Rei Kinjo (NTU Singapore), Joel M. Hawkins (Pfizer), Thomas Knauber (Pfizer), François Lévesque (Merck), Lee Edwards (GSK), and Jean-Philippe Krieger (Syngenta) for helpful discussion.

## REFERENCES

- (1) (a) Crisenza, G. E. M.; Melchiorre, P. Chemistry glows green with photoredox catalysis. *Nat. Commun.* **2020**, *11*, 803. (b) McAtee, R. C.; McClain, E. J.; Stephenson, C. R. J. Illuminating Photoredox Catalysis. *Trends in Chemistry* **2019**, *1*, 111–125. (c) Marzo, L.; Pagire, S. K.; Reiser, O.; König, B. Visible-Light Photocatalysis: Does It Make a Difference in Organic Synthesis? *Angew. Chem., Int. Ed.* **2018**, *57*, 10034–10072. (d) Twilton, J.; Le, C.; Zhang, P.; Shaw, M. H.; Evans, R. W.; MacMillan, D. W. C. The Merger of Transition Metal and Photocatalysis. *Nat. Rev. Chem.* **2017**, *1*, 0052. (e) Shaw, M. H.; Twilton, J.; MacMillan, D. W. Photoredox Catalysis in Organic Chemistry. *J. Org. Chem.* **2016**, *81*, 6898–6926. (f) Romero, N. A.; Nicewicz, D. A. Organic Photoredox Catalysis. *Chem. Rev.* **2016**, *116*, 10075–10166. (g) Schultz, D. M.; Yoon, T. P. Solar Synthesis: Prospects in Visible Light Photocatalysis. *Science* **2014**, *343*, 1239176. (h) Prier, C. K.; Rankic, D. A.; MacMillan, D. W. C. Visible Light Photoredox Catalysis with Transition Metal Complexes: Applications in Organic Synthesis. *Chem. Rev.* **2013**, *113*, 5322–5263. (i) Narayanam, J. M. R.; Stephenson, C. R. J. Visible Light Photoredox Catalysis: Applications in Organic Synthesis. *Chem. Soc. Rev.* **2011**, *40*, 102–113.
- (2) (a) Gisbertz, S.; Pieber, B. Heterogeneous Photocatalysis in Organic Synthesis. *ChemPhotoChem.* **2020**, *4*, 456–475. (b) Ghosh, I.; Khamrai, J.; Savateev, A.; Shlapakov, N.; Antonietti, M.; König, B. Organic Semiconductor Photocatalyst Can. Bifunctionalize Arenes and Heteroarenes. *Science* **2019**, *365*, 360–366. (c) Zhang, Z.; Edme, K.; Lian, S.; Weiss, E. A. Enhancing the Rate of Quantum-Dot-Photocatalyzed Carbon-Carbon Coupling by Tuning the Composition of the Dot's Ligand Shell. *J. Am. Chem. Soc.* **2017**, *139*, 4246–4249. (d) Caputo, J. A.; Frenette, L. C.; Zhao, N.; Sowers, K. L.; Krauss, T. D.; Weix, D. J. General and Efficient C-C Bond Forming Photoredox Catalysis with Semiconductor Quantum Dots. *J. Am. Chem. Soc.* **2017**, *139*, 4250–4253. (e) Kisch, H. Semiconductor Photocatalysis for Chemoselective Radical Coupling Reactions. *Acc. Chem. Res.* **2017**, *50*, 1002–1010.
- (3) (a) Steudel, R.; Chivers, T. The Role of Polysulfide Dianions and Radical Anions in the Chemical, Physical and Biological Sciences, Including Sulfur-Based Batteries. *Chem. Soc. Rev.* **2019**, *48*, 3279–3319. (b) Chivers, T.; Elder, P. J. Ubiquitous Trisulfur Radical Anion: Fundamentals and Applications in Materials Science, Electrochemistry, Analytical Chemistry and Geochemistry. *Chem. Soc. Rev.* **2013**, *42*, 5996–6005.
- (4) Scheers, J.; Fantini, S.; Johansson, P. A Review of Electrolytes for Lithium-Sulphur Batteries. *J. Power Sources* **2014**, *255*, 204–218.
- (5) (a) Zou, Q.; Lu, Y. C. Solvent-Dictated Lithium Sulfur Redox Reactions: An Operando UV-vis Spectroscopic Study. *J. Phys. Chem. Lett.* **2016**, *7*, 1518–1525. (b) Kim, B. S.; Park, S. M. In Situ Spectroelectrochemical Studies on the Reduction of Sulfur in Dimethyl Sulfoxide Solutions. *J. Electrochem. Soc.* **1993**, *140*, 115–122. (c) Leghie, P.; Lelieur, J.-P.; Levillain, E. Comments on the Mechanism of the Electrochemical Reduction of Sulphur in Dimethylformamide. *Electrochem. Commun.* **2002**, *4*, 406–411.
- (6) Roth, H. G.; Romero, N. A.; Nicewicz, D. A. Experimental and Calculated Electrochemical Potentials of Common Organic Molecules for Applications to Single-Electron Redox Chemistry. *Synlett* **2016**, *27*, 714–723.

- (7) (a) Nocera, G.; Murphy, J. A. Ground State Cross-Coupling of Haloarenes with Arenes Initiated by Organic Electron Donors, Formed in situ: An Overview. *Synthesis* **2020**, *52*, 327–336. (b) Smith, A. J.; Poole, D. L.; Murphy, J. A. The Role of Organic Electron Donors in the Initiation of BHAS Base-induced Coupling Reactions between Haloarenes and Arenes. *Sci. China: Chem.* **2019**, *62*, 1425–1438. (c) Lekkala, R.; Lekkala, R.; Moku, B.; Rakesh, K. P.; Qin, H.-L. Recent Developments in Radical-Mediated Transformations of Organohalides. *Eur. J. Org. Chem.* **2019**, *2019*, 2769–2806. (d) Ghosh, I.; Marzo, L.; Das, A.; Shaikh, R.; König, B. Visible Light Mediated Photoredox Catalytic Arylation Reactions. *Acc. Chem. Res.* **2016**, *49*, 1566–1577. (e) Rossi, R.; Lessi, M.; Manzini, C.; Marianetti, G.; Bellina, F. Transition Metal-Free Direct C-H (Hetero)arylation of Heteroarenes: A Sustainable Methodology to Access (Hetero)aryl-Substituted Heteroarenes. *Adv. Synth. Catal.* **2015**, *357*, 3777–3814. (f) Shirakawa, E.; Hayashi, T. Transition-metal-free Coupling Reactions of Aryl Halides. *Chem. Lett.* **2012**, *41*, 130–134.
- (8) (a) Ghosh, I.; Ghosh, T.; Bardagi, J. I.; König, B. Reduction of Aryl Halides by Consecutive Visible Light-Induced Electron Transfer Processes. *Science* **2014**, *346*, 725–728. (b) Ghosh, I.; König, B. Chromoselective Photocatalysis: Controlled Bond Activation through Light-Color Regulation of Redox Potentials. *Angew. Chem., Int. Ed.* **2016**, *55*, 7676–7679. (c) Marzo, L.; Ghosh, I.; Esteban, F.; König, B. Metal-Free Photocatalyzed Cross Coupling of Bromoheteroarenes with Pyrroles. *ACS Catal.* **2016**, *6*, 6780–6784.
- (9) (a) Kim, H.; Kim, H.; Lambert, T. H.; Lin, S. Reductive Electrophotocatalysis: Merging Electricity and Light to Achieve Extreme Reduction Potentials. *J. Am. Chem. Soc.* **2020**, *142*, 2087–2092. (b) Cowper, N. G. W.; Chernowsky, C. P.; Williams, O. P.; Wickens, Z. K. Potent Reductants Via Electron-Primed Photoredox Catalysis: Unlocking Aryl Chlorides for Radical Coupling. *J. Am. Chem. Soc.* **2020**, *142*, 2093–2099.
- (10) (a) Constantin, T.; Zanini, M.; Regni, A.; Sheikh, N. S.; Juliá, F.; Leonori, D. Aminoalkyl Radicals as Halogen-Atom Transfer Agents for Activation of Alkyl and Aryl Halides. *Science* **2020**, *367*, 1021–1026. (b) Constantin, T.; Juliá, F.; Sheikh, N. S.; Leonori, D. A Case of Chain Propagation:  $\alpha$ -Aminoalkyl Radicals as Initiators for Aryl Radical Chemistry. *Chem. Sci.* **2020**, *11*, 12822–12828.
- (11) We observed very weak fluorescence emission around at 480 nm from the DMSO solution of potassium polysulfide ( $K_2S_x$ ). The fluorescence lifetime monitored at 480 nm by the time-correlated single photon counting (TCSPC) in the absence and presence of 4'-bromoacetophenone (**1**) indicated that the excited singlet state of  $S_4^{2-}$  might have photophysical interaction with **1**, that is most likely single-electron-transfer, and thus displayed quenched lifetimes. See the [Supporting Information](#) for more information.
- (12) Takeda, N.; Poliakov, P. V.; Cook, A. R.; Miller, J. R. Faster Dissociation: Measured Rates and Computed Effects on Barriers in Aryl Halide Radical Anions. *J. Am. Chem. Soc.* **2004**, *126*, 4301–4309.
- (13) Another photoredox cycle by the single redox couple of  $S_4^{2-}/S_4^{\bullet-}$ , where a ground state  $S_4^{\bullet-}$  oxidizes the radical intermediate **III** to form product **3** along with the regeneration of  $S_4^{2-}$ , is not completely ruled out as the mechanistic possibility.
- (14) (a) Chivers, T. Ubiquitous Trisulphur Radical Ion  $S_3^{\bullet-}$ . *Nature* **1974**, *252*, 32–33. (b) Zhang, G.; Yi, H.; Chen, H.; Bian, C.; Liu, C.; Lei, A. Trisulfur Radical Anion as the Key Intermediate for the Synthesis of Thiophene via the Interaction between Elemental Sulfur and NaOtBu. *Org. Lett.* **2014**, *16*, 6156–6159.
- (15) Breder, A.; Depken, C. Light-Driven Single-Electron Transfer Processes as an Enabling Principle in Sulfur and Selenium Multicatalysis. *Angew. Chem., Int. Ed.* **2019**, *58*, 17130–17147.
- (16) Dean, J. A. *Lange's Handbook of Chemistry*, 15th Ed.; McGraw-Hill, Inc.: New York, 1992.
- (17) (a) Liu, B.; Lim, C.-H.; Miyake, G. M. Visible-Light-Promoted C-S Cross-Coupling Via Intermolecular Charge Transfer. *J. Am. Chem. Soc.* **2017**, *139*, 13616–13619. (b) Crisenza, G. E. M.; Mazzarella, D.; Melchiorre, P. Synthetic Methods Driven by the Photoactivity of Electron Donor-Acceptor Complexes. *J. Am. Chem. Soc.* **2020**, *142*, 5461–5476.
- (18) Bailey, T. S.; Henthorn, H. A.; Pluth, M. D. The Intersection of NO and  $H_2S$ : Persulfides Generate NO from Nitrite through Polysulfide Formation. *Inorg. Chem.* **2016**, *55*, 12618–12625.
- (19) (a) Wallace, T. J.; Mahon, J. J. Reactions of Thiols with Sulfoxides. II. Kinetics and Mechanistic Implications. *J. Am. Chem. Soc.* **1964**, *86*, 4099–4103. (b) Wallace, T. J. Reactions of Thiols with Sulfoxides. I. Scope of the Reaction and Synthetic Applications. *J. Am. Chem. Soc.* **1964**, *86*, 2018–2021. (c) Yiannios, C. N.; Karabinos, J. V. Oxidation of Thiols by Dimethyl Sulfoxide. *J. Org. Chem.* **1963**, *28*, 3246–3248.
- (20) Andrieux, C. P.; Blocman, C.; Dumas-Bouchiat, J. M.; M'Halla, F.; Savéant, J. M. Determination of the Lifetimes of Unstable Ion Radicals by Homogeneous Redox Catalysis of Electrochemical Reactions. Application to the Reduction of Aromatic Halides. *J. Am. Chem. Soc.* **1980**, *102*, 3806–3813.
- (21) Costentin, C.; Robert, M.; Savéant, J.-M. Fragmentation of Aryl Halide  $\pi$  Anion Radicals. Bending of the Cleaving Bond and Activation vs Driving Force Relationships. *J. Am. Chem. Soc.* **2004**, *126*, 16051–16057.
- (22) Connell, T. U.; Fraser, C. L.; Czyn, M. L.; Smith, Z. M.; Hayne, D. J.; Doeven, E. H.; Agugiaro, J.; Wilson, D. J. D.; Adcock, J. L.; Scully, A. D.; Gomez, D. E.; Barnett, N. W.; Polyzos, A.; Francis, P. S. The Tandem Photoredox Catalysis Mechanism of  $[Ir(ppy)_2(dtbbpy)]^+$  Enabling Access to Energy Demanding Organic Substrates. *J. Am. Chem. Soc.* **2019**, *141*, 17646–17658.
- (23) Pause, L.; Robert, M.; Savéant, J.-M. Can Single-Electron Transfer Break an Aromatic Carbon-Heteroatom Bond in One Step? A Novel Example of Transition between Stepwise and Concerted Mechanisms in the Reduction of Aromatic Iodides. *J. Am. Chem. Soc.* **1999**, *121*, 7158–7159.
- (24) Li, P.; Meng, G.; Chen, K.; Wang, L. Recent Advances in Transition-Metal-Free Aryl C-B Bond Formation. *Synthesis* **2017**, *49*, 4719–4730.
- (25) (a) Jin, S.; Dang, H. T.; Haug, G. C.; He, R.; Nguyen, V. D.; Nguyen, V. T.; Arman, H. D.; Schanze, K. S.; Larionov, O. V. Visible Light-Induced Borylation of C-O, C-N, and C-X Bonds. *J. Am. Chem. Soc.* **2020**, *142*, 1603–1613. (b) Jiang, M.; Yang, H.; Fu, H. Visible-Light Photoredox Borylation of Aryl Halides and Subsequent Aerobic Oxidative Hydroxylation. *Org. Lett.* **2016**, *18*, 5248–5251.
- (26) (a) MacKenzie, I. A.; Wang, L.; Onuska, N. P. R.; Williams, O. F.; Begam, K.; Moran, A. M.; Dunietz, B. D.; Nicewicz, D. A. Discovery and Characterization of an Acridine Radical Photoreductant. *Nature* **2020**, *580*, 76–80. (b) Bardagi, J. I.; Ghosh, I.; Schmalzbauer, M.; Ghosh, T.; König, B. Anthraquinones as Photoredox Catalysts for the Reductive Activation of Aryl Halides. *Eur. J. Org. Chem.* **2018**, *2018*, 34–40. (c) Discekici, E. H.; Treat, N. J.; Poelma, S. O.; Mattson, K. M.; Hudson, Z. M.; Luo, Y.; Hawker, C. J.; de Alaniz, J. R. A Highly Reducing Metal-Free Photoredox Catalyst: Design and Application in Radical Dehalogenations. *Chem. Commun.* **2015**, *51*, 11705–11708. (d) Kim, H.; Lee, C. Visible-Light-Induced Photocatalytic Reductive Transformations of Organohalides. *Angew. Chem., Int. Ed.* **2012**, *51*, 12303–12306. (e) Nguyen, J. D.; D'Amato, E. M.; Narayanam, J. M.; Stephenson, C. R. Engaging Unactivated Alkyl, Alkenyl and Aryl Iodides in Visible-Light-Mediated Free Radical Reactions. *Nat. Chem.* **2012**, *4*, 854–859.
- (27) The quantum yields for the borylation and hydrodebromination of **1** were determined as 0.48 and 0.21, respectively. While these values support the photoredox mechanism, a contribution of the radical chain processes to the product formation may be involved to some extent. See the [Supporting Information](#) for details.
- (28) Cambié, D.; Bottecchia, C.; Straathof, N. J. W.; Hessel, V.; Noël, T. Applications of Continuous-Flow Photochemistry in Organic Synthesis, Material Science, and Water Treatment. *Chem. Rev.* **2016**, *116*, 10276–10341.